COMMISSIONING OF NSLS-II*

F. Willeke, BNL, Upton, NY 11973, USA

Figure 1: Aerial view of NSLS-II.

Abstract

NSLS-II, the new 3rd generation light source at BNL was designed for a brightness of 10^{22} photons s^{-1} mm^{-2} $mrad^{-2}$ $(0.1\%BW)^{-1}$. It was constructed between 2009 and 2014. The storage ring was commissioned in April 2014 which was followed by insertion device and beamline commissioning in the fall of 2014. All ambitious design parameters of the facility have already been achieved except for commissioning the full beam intensity of 500mA which requires more RF installation. This paper reports on the results of commissioning.

NSLS-II OVERVIEW

The NSLS at BNL was the pioneer of the 3rd Generation Light Sources which provided a wealth of scientific results which have shaped the landscape of synchrotron radiation based science. However, the high demands on the performance of synchrotron light sources in the future motivated constructing a new machine which would enable spatial resolution of 1 nm and energy resolution of 0.1 meV. This mission was acknowledged by the Department of Energy in 2005 when the design of the new machine began. The goals require a beam brightness of B = 10^{22} photons s^{-1} mm^{-2} $mrad^{-2}$ $(0.1\%BW)^{-1}$. The corresponding beam parameters are a beam current of 500 mA, a sub-nm horizontal emittance with < 1% emittance ratio. Furthermore, state-of- the- art and beyond small gap undulators are needed to generate the ultra-bright photon beams. With full beam intensity, NSLS-II will be the brightest synchrotron at present.

The facility has the following topology: The ~800 m circumference ring building houses the accelerator tunnel (width 3.7m, height 3.2m) and the 17m wide experimental floor. Power supplies, vacuum equipment, diagnostics and controls are placed on the 86 cm thick tunnel roof. The ratchet shield wall is 100 cm thick.

* Work supported by DOE under contract No.DE-AC02-98CH10886.

The injector complex with the 200 MeV s-band LINAC and the 158 m circumference 3 GeV Booster Synchrotron is placed inside the ring. Also on the inside of the ring are five service buildings with mechanical utilities and HVAC systems as well as the RF-Cryogenic complex. The cooling tower and the central DI water system are in the center of the ring. On the outside of the ring building are five laboratory-office- buildings, each with 145 seats and several laboratory spaces. (See Figure 1.)

ACCELERATOR LATTICE

NSLS-II has a double bend achromat lattice with 30 cells on a 792 m circumference. The dipole magnets are long and weak (l = 3.69 m, B = 0.4 tesla) which allows obtaining close to DBA minimum beam emittance with moderate peak beta-values (30 m) and chromaticities >- 3. The gentle bends also imply low energy loss per turn (286 keV/e/turn). These are favorable conditions to increase radiation damping by adding six 3.4m long, 1.85 Tesla damping wigglers thereby increasing radiation damping and reducing emittance by more than a factor of two. The beam emittance obtained this way is only 0.9 nm rad. The straight sections for insertion devices alternate between long (9.3m, 3m vertical beta) and short (6.6m, 1m vertical beta). The damping wigglers weakly break the 15-fold symmetry to 3-fold symmetry. Three of the long straight sections are needed for injection and six superconducting RF cavities (including two passive units; for details see [1].)

TIMELINE

The mission of NSLS-II was acknowledged in 2005 by the DOE (CD-0) which was followed swiftly by the completion of the conceptual design and the establishment of a cost and schedule baseline (CD-1 in 2007 and CD-2 in 2008). Civil construction started in June 2009 after CD-3 was granted. Two years later, in the spring of 2011, the first part of the ring building was ready for accelerator installation which was completed by

ISBN 978-3-95450-168-7

the end of 2013. Meanwhile the injector had been installed and tested, and the LINAC was commissioned in April 2012. The Booster commissioning followed in December 2013. On 26 March 2014, authorization for storage ring commission was obtained and storage ring commissioning started with a normal conducting 7-cell 500 MHz cavity. Commissioning was completed by mid-May 2014. During the summer of 2014, the first suite of insertion devices and the superconducting cavity was installed. A beam current of 50mA was stored.

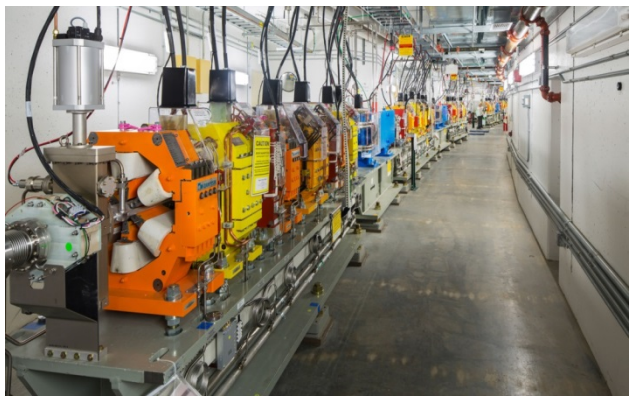

Figure 2: View of one NSLS-II DBA cell.

Operation of the NSLS-II accelerators started on October 1st 2014 with commissioning of the insertion devices, the beam line front end and the six beam lines which were funded by the NSLS-II project. This was completed by the end of 2014. Operation for beam lines started in February 2015. During regular machine studies, the performance of the accelerator complex was steadily improved. By the end of April, 200 mA of beam current was demonstrated and all other design parameters of NSLS-II had been achieved.

BRIEF DESCRIPTIONS OF SUBSYSTEMS

The accelerator magnets of NSLS-II are conventional electro-magnets. All 300 quadrupole magnets are individually powered by switched mode power supplies. Sextupole magnets are powered in 9 circuits in each of the five pentants. Correctors include iron yoke dipole correctors, correction windings on dipole coils, air coil-skew and -fast dipole correctors. The vacuum system is made of extruded, keyhole-shaped Al and has distributed NEG strip pumps in the antechambers. The power is delivered to the beam by up to four (one at present) superconducting single cell 500 MHz cavities (CESR-B type). The RF power is generated by klystron transmitters. The full suite of beam diagnostics includes the in-house developed BPM system with 200 nm resolution and stability. The control system is based on EPICS. Special features are the high-level-application platform which is well integrated in the middle-layer and the deterministic 10 kHz data link for real time feedback and time critical equipment protection. The six, 3.4 m long damping wigglers are permanent magnets (NeFeB) with permadure poles (1.85 Tesla peak field). The majority of the insertion devices are permanent magnets in-vacuum-undulators (IVU) with 5 mm gap height and period lengths of 20-23 mm. All power supply, vacuum controls, diagnostics, and controls are housed in air-cooled, sealed racks which provide a friendly environment for sensitive and highly reliable equipment.

INJECTOR SYSTEM

The NSLS-II injector consists of a 200 MeV s-band LINAC and a 3 GeV combined function booster synchrotron. The Linac has three solid state modulators (including the hot spare) which drive the four accelerating units. The electron source is a thermionic gun followed by a 500 MHz pre-buncher and an s-band buncher structure. The linac is operated with a maximum charge of 15 nC/s. The linac has two beam dumps, one for the linac itself and another one after the energy spectrometer in the linac to booster transfer line. The system was commissioned in April 2012. The booster is a combined function machine with 60 focusing/defocusing dipoles. The circumference is 158 m. The cycle time is 1 sec. With additional quadrupole magnets at both ends of the four arc sections, a horizontal emittance of 35 nm has been achieved. RF power is delivered to the beam by a PETRA 7-cell 500 MHz Cu-cavity driven by a 90 kW IOT based transmitter system. Injection is accomplished by a two-kicker bump and extraction pulsed magnets are supported by a slow extraction bump system. A high energy transfer line with a 3GeV beam dump connects to the storage ring injection straight. The booster has very flexible EPICs based controls and has a full suite of instrumentation (BPMs with turn by turn capacity, tune monitor, optical monitor, intensity monitors) which enabled a very fast commissioning. Within three weeks acceleration of a beam to 3 GeV could be demonstrated and only two weeks later, a transmission of close to 100% was achieved routinely [10]. The injector complex is very robust. After a break or shutdown, full performance is re-established after only a few hours. Operation is fairy reliable and re-tuning is required only rarely.

STORAGE RING COMMISSIONING

Overview

Storage ring commissioning started on 26 March 2014. The beam was stored after a few days. The excellent stretched wire alignment of quadrupole magnets w.r.t. the other six multipole magnets on the same girder of less than 10 μm and initial on-axis injection were important factors in the fast initial commissioning. (See Figure 2.)

Accumulation of 25 mA was achieved after orbit and chromaticity correction. Up to this point, commissioning was performed with a PETRA 7-cell 500 MHz Cu-cavity. In a shutdown in May/June 2014 the first superconducting cavity was installed and 50 mA of beam current was demonstrated with superconducting cavities shortly after restart of commissioning. Commissioning was concluded by July 10th after less than 50 days of commissioning. It

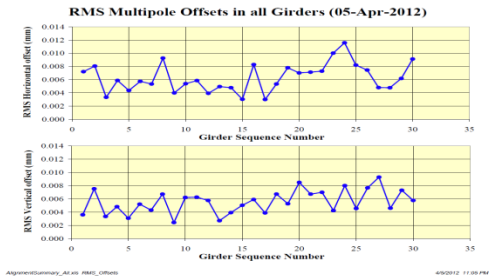

Figure 2: RMS values of magnet offsets w.r.t. an ideal straight line on magnet girders of NSLS-II.

should be mentioned that the excellent instrumentation and the fact that high level applications were fully integrated into the control system from day one were important factors in this quick success. Operation of NSLS-II started on October 1st 2014 with the commissioning of insertion devices, beam line front ends and beam lines. For all eight insertion devices and six beam line frontends commissioning was completed by the end of 2014 and all six initial beam lines received "first light" within this period.

Figure 3: Celebration of "first Light" in the CSX beam line on October 23 2014.

Lattice Commissioning

The rms quadrupole magnet gradient errors in NSLS-II are $\Delta G/G = 0.1\%$. Each quadrupole can be individually adjusted. The sextupole alignment error is ~10 μm. These values are an excellent base for lattice commissioning and small residual errors. The most important tool for the lattice commissioning is the BPM system. The NSLS-II BPM system has turn-by-turn (TbT) capability with an rms noise of ~2 μm. Average (38 turns) BPM readings have a 200 nm resolution and stability and are provided with 10 kHz data rate. The beam optics functions have been measured with various response matrix techniques ($R= \Delta z_j/\Delta\theta_i$, z_j are beam coordinates and θ_i are correction magnet kicks) and the program "LOCO" (see [2]) and have been corrected by least square minimization techniques to better than $\Delta\beta/\beta = 3\%$. The dispersion functions after correction differ by only a few millimeters from the design values (zero in the vertical case). Corrections show that gradient errors are randomly distributed. Closed orbit errors have a large impact on beta-beats and iterative orbit and optics corrections were needed. Cycling magnets (including correctors) in a consistent way is important to maintain good orbits and beam optics. Global and local x-y coupling is determined by TbT BPM measurements and by deriving the mode-II horizontal and the mode-I vertical beta functions [3,4,5] from the measured revolution matrices. There is one skew quadrupole corrector in each cell which allows an almost perfect correction of the coupling (see Figure 4).

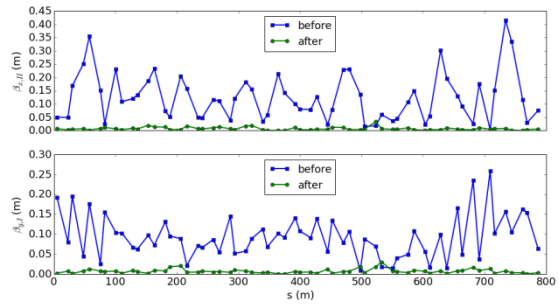

Figure 4: Local and global coupling correction: the mode-II β_{xII} and mode-I β_{yI} which represent the off diagonal blocks of the 4x4 revolution matrices at each element of the accelerator before and after correction.

After optics corrections, the half integer stop bands can be crossed without beam loss. See Figure 5.

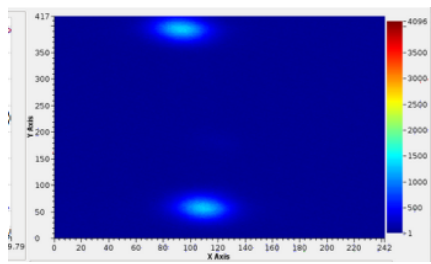

Figure 5: NSLS-II beam stored within the vertical ½ integer resonance stop-band shown by the synchrotron light monitor.

The horizontal beam emittance of NSLS-II is designed to be 2nm rad for the bare lattice. With 20.4 m of damping wigglers (gap 15 mm, period 100 mm and peak field 1.85 Tesla, six 3.4 m long units installed in pairs in three equally spaced straight sections) the value drops to 0.9π nm rad. This has been confirmed by measurements (see Figure 6). After careful correction of vertical dispersion and coupling, the vertical emittance as measured with the pin-hole X-ray monitor is as low as 6π pm rad which is well below the already diffraction limited (2 keV photons) design value.

Orbit Stabilization

NSLS-II beam orbits are quite stable even without active stabilization. The magnet support system does not amplify the ground vibrations at the level of up to 100 nm and all rotating equipment is well isolated from the storage ring tunnel floor. The horizontal orbit varies by about 2 microns which is less than the specification of 10% of the beam size. The vertical motion is about 0.6

ISBN 978-3-95450-168-7

micron, a factor of two above the specification which requires active stabilization. A fast orbit feedback system has been implemented using the fast deterministic data link (10 kHz BW) and FPGA based controllers, one in each cell, which receives all BPM data and calculates changes for the air-coil correction dipoles. The feedback algorithm corresponds to the well proven NSLS orbit stabilization system [8]. With active stabilization, the residual beam motion is well within the specification. However the system is not yet fully optimized for routine operations.

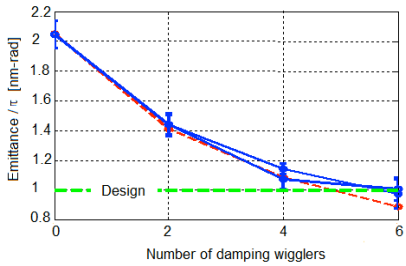

Figure 6: Measurement of horizontal emittance vs. number of damping wigglers with a pin-hole X-ray monitor (blue: measurements, red: calculation)

Dynamic Aperture

In a low emittance lattice, the dynamic aperture is compromised by the small dispersion which requires strong sextupoles to compensate the high chromaticity. NSLS-II has three chromatic sextupole families and six families at locations with zero linear dispersion to compensate the nonlinear field effects which are higher order chromaticity and tune shift with amplitude as well as driving terms of non-linear resonances. A well-established method to probe the stability by simulation is to generate a frequency map [7]. Particles are launched into phase space at the injection point and the variation of the betatron tunes on their travel around the accelerator is recorded. The result of this procedure is visualized by plotting the corresponding rms tune changes color coded on each starting point in phase space. Such a frequency map shows clearly the boundary of stability and resonances within the aperture. During commissioning, the beam was launched on trajectories in the entire range of physical aperture by firing fast kicker magnets in each plane. The trajectory with the largest amplitude and no beam loss is interpreted as the border of stability. Figure 7 shows a typical simulation for the NSLS-II bare lattice and the corresponding experimental results are plotted in Figure 8. We conclude that the measured dynamic aperture of NSLS-II is very close to simulated values. The most important benefit of sufficient dynamic aperture is an injection efficiency of 100% and reasonable margin in dynamic aperture for insertion device commissioning.

High Intensity Commissioning

A large effort has been spent during the design of NSLS-II in calculating the impedance of all vacuum devices [11]. The single bunch intensity in NSLS-II is limited by transverse mode coupling instability in the vertical plane at I_b=0.95 mA (bare lattice, $\xi_{x,y}$ = 0; with $\xi_{x,y}$ = 5, I_b = 3 mA) which can be concluded from the significant tune change as a function of bunch intensity. The bunch becomes unstable if the tune shift reaches half the synchrotron tune. The calculations predict a threshold of 1.5 mA with 10 insertion devices. This is not yet understood. The threshold for the micro-bunch instability is calculated to be 9 mA [7]. The longitudinal bunch stability is demonstrated up to 6 mA. However the bunch lengthening by potential well distortion is also larger than expected (see Figure 9) which needs to be understood.

The NSLS-II design beam current is 500 mA which is close to the expected multibunch instability limit due to resistive wall impedance in the 5 mm gap insertion devices. A broad band (250 MHz) transverse damper system has been installed to actively stabilize the beam if required. However we observe that at nominal values of the chromaticity of ξ_{xy} = +2, the onset of transverse instability is observed at currents above 50 mA. The observed multibunch modes of unstable beam cluster around m = 0. Head tail damping from chromaticities > +2 can stabilize the beam up to 150 mA. It is observed that the onset of stability can be shifted to larger beam intensity if the bunch train is split in up to six sub-trains. This is interpreted as an indication of the presence of fast ion instability [9]. Beam is kept stable by active damping.

.

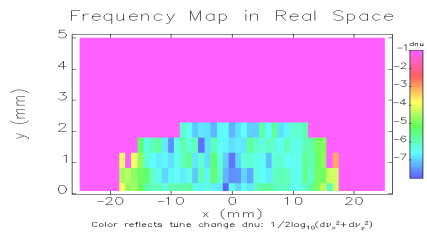

Figure 7: Frequency map of NSLS-II Dynamic Aperture (DA) in the x-y plane at injection point.

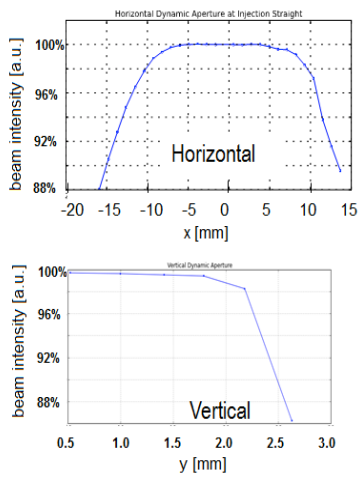

Figure 8: Probing the NSLS-II DA by kicking the beam with a fast kicker (same reference point as above).

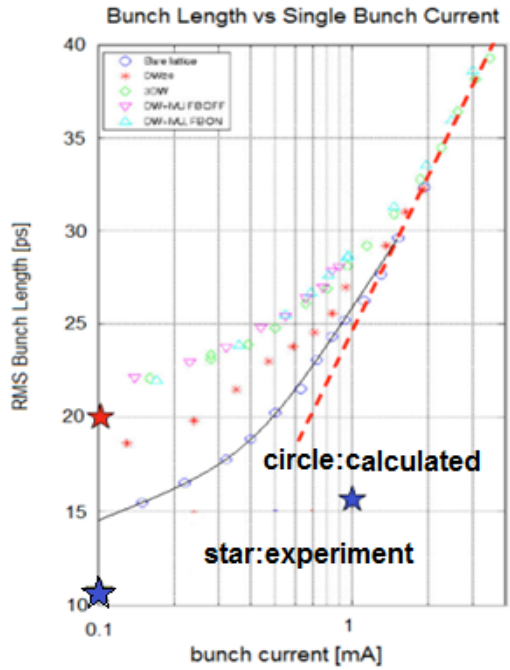

Figure 9: Measured and expected bunch lengthening in NSLS-II.

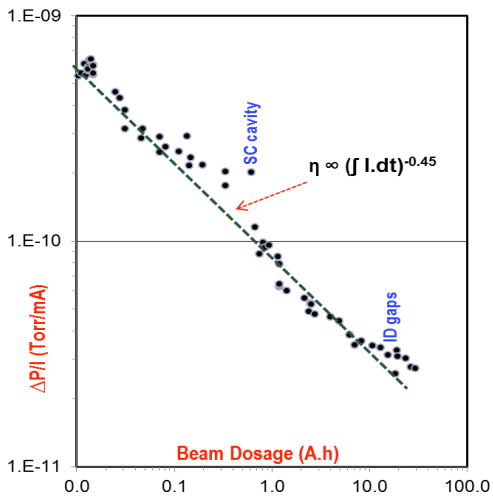

Figure 10: Improvement of dynamic pressure rise with beam current.

At this point a maximum beam intensity of up to 200 mA has been stored. Vacuum performance is improving steadily. Figure 10 shows the improvement of dynamic average pressure rise with integrated beam current.

Insertion Device Commissioning

The first suite of NSLS-II insertion devices includes the six damping wigglers, two 3 m long in vacuum undulators (IVU) with λ=20 mm period g=5 mm gap (peak field of 1.2Tesla), a 3m long wide pole IVU with λ=22 and g=5 mm, a 1.5 m long λ=21 mm g=5mm IVU and a pair of 2m long λ=49 mm elliptical polarizing undulators (EPU). The impact of all undulators on the beam is small. Residual tune and orbit changes can be easily corrected for and feed forward tables converged quickly. The damping wigglers require local optics correction and global tune correction. The residual effects after corrections are small. The dynamic aperture is only slightly affected by the insertion devices provided that the beam orbit is carefully centered in the small gap undulators [12].

SUMMARY

Table 1 summarizes the present state of NSLS-II performance. All design parameters (except the beam intensity) have already been achieved or have been exceeded. Full beam intensity of 500 mA requires the 2nd superconducting cavity is installed which is planned later this year. NSLS-II is designed for Top-Off mode of injection which will be available by October 2015.

Table 1: NSLS-II Design and Current Parameters

Parameter	Design	Current
Beam Energy [GeV]	3	3
Beam Current [A]	0.5	0.2
Beam Emittance h [nm rad]	0.9	0.9
Beam Emittance h [pm rad]	8	6
Orbit stability [beam size]	10%	<10%
Relative Energy Spread	0.04%	0.04%
Dynamic Aperture h, v [mm]	>15,>2.5	15, 2.5

CONCLUSION

NSLS-II, the ultimate 3 GeV 3rd Generation Light Source has been successfully completed and commissioning went very smoothly. All design parameters have been achieved or exceeded except for the peak intensity which will require an additional superconducting RF cavity. More work is required to understand collective effects and to achieve the required stability and reproducibility in routine operations. The performance of the machine is very stable and mature at this early stage. Operation for beam line users has started.

ACKNOWLEDGMENT

The successful construction and commissioning of NSLS-II is the result of the hard work of the entire very committed, high-skilled NSLS-II staff. The author is indebted to Satoshi Ozaki for advice and support during construction of NSLS-II.

REFERENCES

[1] F. Willeke, TUOS3, PAC'11, New York, 2011
[2] J. Safranek, Nucl. Inst. And Meth. A388, 27 (1997)
[3] G. Ripken, F. Willeke, AIP Conf. Proc. 184 (1989)

ISBN 978-3-95450-168-7

[4] V. Lebedev and A. Bogacz, arXiv:1207.5526
[5] Y. Li, these proceedings, IPAC'15, Richmond, Virginia, USA (2015)
[6] J. Laskar, Physica D: Nonlinear Phenomena, 1993
[7] A. Blednykh, S. Krinsky, B. Nash, L.H. Yu, FR5RFP033, PAC'09, Vancouver
[8] Li Hua, L.H. Yu, E. Bomki, J. Galayda, S. Krinsky, G. Vignola, Nucl. Instr. Meth. A *284,* (1989)
[9] T. Raubenheimer, F. Zimmermann, SLAC–PUB95–6740
[10] E. Blum et al., TUPMA050, IPAC15, Richmond, Virginia, USA (2015)
[11] A. Blednykh et al., TUAB2, IPAC15, Richmond, Virginia, USA (2015)
[12] G. Wang et al., MOPJE053, IPAC15, Richmond, Virginia, USA (2015)